N64-33921
(ACCESSION NUMBER)   (THRU)
_46_
(PAGES)
_CR 59369_
(NASA CR OR TMX OR AD NUMBER)
_/_
(CODE)
_25_
(CATEGORY)

SUMMARY REPORT

INVESTIGATION OF CURRENT

DEGRADATION PHENOMENON

IN SUPERCONDUCTING SOLENOIDS

June 1963 - May 1964

L. C. Salter, Jr.

OTS
XEROX $ _2.00_
MICROFILM $ _.50_

CONTRACT NAS8-5356

MARSHALL SPACE FLIGHT CENTER

HUNTSVILLE, ALABAMA

SUMMARY REPORT

INVESTIGATION OF CURRENT
DEGRADATION PHENOMENON
IN SUPERCONDUCTING SOLENOIDS

June 1963 - May 1964

L. C. Salter, Jr.

CONTRACT NAS8-5356

MARSHALL SPACE FLIGHT CENTER

HUNTSVILLE, ALABAMA

ABSTRACT

33921

Various aspects of the current degradation phenomenon in superconducting solenoids have been investigated. Critical currents of unplated 0.025 cm dia Nb-25%Zr wire are found to depend on the center-to-center spacing of the wires and on the number of layers of solenoid winding. For copper-plated 0.025 cm dia Nb-Zr wires, solenoid critical currents are found to be given by $I = I_1 \log l + I_2$, where l is the wire length. Solenoid currents can be predicted to better than $\pm 10\%$ for both classes of wires. Experiments with various diameter Nb-33%Zr wires show that for copper-plated and unplated wires both solenoid and short sample critical currents decrease with increasing diameter. Degradation also increases with diameter. The effects of mechanical constraint and thermal environment are minor. SN transition investigations show that the normal transition originates in the highest field region in the experimental solenoid and propagates predominantly by a process other than joule heating. Short sample tests are found to produce super-current instabilities which are sensitive to dH/dt. These instabilities, which depend on manufacturing process and supplier, could not be correlated with post-cold-work metallographic examinations.

1

CONTENTS

FIGURES

3

TABLES

I. INTRODUCTION

Current degradation in superconducting solenoids is the phenomenon where-by superconducting wires carry less super-current when wound in solenoidal form than when tested as isolated short samples. This phenomenon is illustrated in Figure 1 for 0.025 cm dia Nb-25%Zr. The upper curve shows short-sample critical current, I_c, versus transverse, applied field. Solenoid critical currents, I_s, as a function of self-field are significantly lower than I_c and lie in the shaded area. Our principal investigations of this degradation have included: the effects of solenoid geometrical parameters; correlations between short sample and solenoid currents; the variations of short sample and solenoid currents with wire diameter; and the location and propagation of superconducting to normal (SN) transitions in solenoids. Results of these studies are discussed in detail in the text. During the course of work, qualitative information on the influence of thermal environment and mechanical constraint on solenoid currents was obtained and is briefly discussed.

The above investigations were limited to the Nb-Zr system. Unless other-wise stated, the results are 0.025 cm dia wire.

II. INFLUENCE OF GEOMETRICAL PARAMETERS ON SOLENOID CRITICAL CURRENT

A. UNPLATED WIRE SOLENOIDS

We have investigated the effect of geometrical parameters on the critical current, I_s, for <u>unplated</u> Nb-25%Zr wire solenoids. We find an empirical dependence of I_s on the number of layers of winding, N_r, and on the center-to-center spacings of wires in the axial and radial directions, S_z and S_r, respectively.

Critical currents for several solenoids are plotted as a function of N_r in Figure 2. The solid line, I_s' <u>versus</u> N_r, represents the average values of I_s at any N_r. The scatter of $\pm 18\%$ in I_s about the I_s' curve for $N_r > 20$ is primarily due to variations in S_z and S_r. This dependence of I_s on S_z and S_r is found by plotting I_s/I_s', for the proper N_r, against S_z or S_r for each data point. This curve can be extrapolated to find I_o/I_s' at $S_z = S_r = $ do $= 0.028$ cm. I_o is the current for touching, <u>uninsulated</u> wires. These results are shown in Figure 3 except the ordinate has been normalized to I_s/I_o.

Differences between the effect of S_z and S_r were not detected. Also, the above procedure neglects any effect of N_r on the results shown in Figure 3. Certainly, some of the remaining scatter could be due to N_r, but there is insufficient data to resolve this question.

Figure 3 shows that I_s increases with an increase in wire spacing, but that this increase becomes relatively small after a spacing of one and one-half to two wire diameters is reached. The decrease in winding density due to an increase in spacing is greater than the gain in I_s. Thus, it is more efficient to wind a solenoid as tightly as possible.

Figures 2 and 3 can be used to generate a third curve, I_o <u>versus</u> N_r. To find I_o for each solenoid, the actual solenoid current (I_s from Figure 2) is divided by the two values of I_s/I_o (Figure 3) for the S_r and S_z of the solenoid. The dashed line in Figure 3 is used to approximate I_s/I_o. The following example best serves to illustrate the procedure. For coil #16 in Table I, $I_s = 19.2$A and

$N_r = 52$. From Figure 3, $I_s/I_o = 1.24$ and 1.14 for $S_z = 0.0406$ cm and $S_r = 0.0340$ cm, respectively. Then $I_o = \dfrac{19.2}{(1.24)(1.12)} = 13.8A$, which is shown in Figure 4.

Two additional comments are in order. First, N_r and the self-generated magnetic field are related, and N_r is used primarily for convenience. Secondly, this correlation is valid for a range of solenoid geometries as can be seen by examining the geometrical parameters in Table I. In particular, solenoids Nos. 1 and 20 represent the geometrical extremes with $a_1 = 0.63$ cm, $\alpha = 1.02$, $\beta = 2.0$, and $a_1 = 3.46$ cm, $\alpha = 1.23$, $\beta = 2.53$, respectively. This critical currents of these two coils are consistent with the above results.

Therefore, for <u>unplated</u> wire, solenoid critical currents are related to the spacing of wires (Figure 3), and the number of layers of winding (Figure 4). These results, in particular those in Figure 4, are sensitive to alloy percentage and manufacture and cannot be considered universal although the qualitative results should be generally valid.

B. COPPER-PLATTED WIRE SOLENOIDS

Copper-plated wire solenoids carry considerably higher currents than unplated wire coils, and in some cases short sample currents are achieved. I_s for plated-wire coils is found to obey the following empirical relationship:

$$I_s = I_1 \log(\ell) + I_2 \tag{1}$$

where
ℓ = length of wire

I_1 and I_2 are constants

Data for several coils are shown in Figure 5. For all but one of the curves, a_1 and β are held constant and while ℓ and, therefore, α vary. * In Figure 5 for the Avco solenoids, α and β are constant while ℓ and α are varied. In both

---

* For a solenoid of rectangular winding cross section, a_1, a_2, and $2b$ are the inner radius, outer radius, and axial length, respectively, of the windings. $\alpha = a_2/a_1$ $\beta = b/a_1$.

cases the critical currents obey Equation 1. The slope I_1 is constant for all curves, but I_2 depends on the a_1, α and β of a coil and on alloy percentage. Thus, I_1 is known from Figure 5 for 0.025 cm dia Nb-Zr wire, but I_2 must be experimentally determined. Equation 1 appears accurate to ± 5%. One might expect that the curve of I_s in Figure 5 would become approximately constant at 15A as in Figure 2. These results for plated wire should be quite useful in solenoid design since Equation 2 seems dependent on alloy percentage and manufacture through the constant I_2, which can be experimentally determined.

The reason that some solenoids carry short sample currents can be seen from the following arguments. For any solenoid I_c and I_s can be predicted from Figures 1 and 5, respectively. Whenever $I_c < I_s$, then the solenoid will operate on the short-sample H-I_c curve. Such operation can result only for certain solenoid geometries and wire lengths: the wire length is the order of meters for low values H and reaches a maximum length of 3000m to 5000m at 60 kG to 70 kG.

III. CORRELATIONS BETWEEN SHORT SAMPLE AND SOLENOID CURRENTS

A. SHORT SAMPLE AND SOLENOID TESTS

The purpose of this work was to correlate short sample tests with solenoid critical currents and to investigate variations in short-sample and solenoid current behavior due to material processing. Four series of tests were conducted on 0.025 cm dia Nb-25%Zr and Nb-33%Zr wires from four suppliers. The tests are described below.

1) Standard Short Wire H-I Tests - The sample current is increased in a constant, transverse field.

2) Inverse Short Wire H-I Tests - The sample current is held constant while H is increased or decreased with constant $\frac{dH}{dt}$.

3) Coil Simulation Tests - The external field is increased in proportion to short sample current, H/I = constant, to simulate solenoid behavior.[1]

4) Solenoid Tests - Solenoids were constructed with 800m each of the various wires.

In the short sample tests the wires were mounted in hair-pin fashion, potted in Emerson and Cuming Stycast 2850 FT epoxy, and protected from damage due to ohmic heating with a shunt.

B. RESULTS

Characteristic results are discussed below and presented in Figures 6-11.

1. Standard H-I Test

This test defines a unique maximum critical current curve for each sample.

2. Inverse H-I Test

This test causes super-current instabilities (SN transitions) at field-current values well below the standard H-I curve (Test #1 above) for the wires shown in Figures 6-10. The horizontal dashed lines show the current-field

history. The series of triangles with subscripts indicate the sequence of transitions. These successive transitions result from repeating the inverse H-I test starting at the field of the last transition. The resulting unstable region is bounded between ~ 5 and ~ 30 kG in field and between the standard H-I curve and some minimum current, I_m, in the 15 to 30A region.

3. Coil Simulation Tests

Super-current instabilities also are observed in the simulation tests. In the figures, the H/I = constant paths are represented by the slanted, dashed lines. The subscripts indicate the sequence of the tests at each value of H/I. Each successive test necessarily begins at the H = I = O condition. Transitions in this test define essentially the same unstable regions as in the inverse H-I tests. Since the only difference between the two experiments is the presence of a dI/dt in the simulation test, it is concluded that dI/dt does not affect the results.

4. Solenoid Tests

The critical currents of solenoids constructed with the above wires are shown in the appropriate figures and are tabulated with other solenoid parameters in Table II.

C. DISCUSSION

Different wires exhibit varying degrees of the super-current instability as seen in Tests #2 and #3 above. Judging this degree is somewhat qualitative; but, in general, stability increases with the magnitude of I_m. Thus, Figures 6, 7, and 8 are for very unstable wire since $I_m \approx$ 20A. Figures 9 and 10 show semi-stable behavior because I_m has increased to 25-30A. Finally, Figure 11 presents results for very stable wire which only goes normal at the standard H-I curve.

We have also noticed that the number of SN transitions experienced in transversing the unstable region, defined here as N_t, is dependent on dH/dt for the semi-stable wires. For dH/dt $\approx$ 100 gauss/sec, N_t reduces to one or two transitions, but increases to 5 or 6 for dH/dt $\approx$ 1200 gauss/sec. In the very unstable wires, N_t is large (> 6) regardless of the magnitude of dH/dt.

Conversely, it is felt that the stable wire in Figure 11 could be driven normal if dH/dt were sufficiently large.

An important result is that critical currents of solenoids constructed with these wires reflect the stability found for short samples provided that the wires are copper-plated. In particular, for solenoids C-105, C-106, C-108, and C-109, constructed with semi-stable and stable plated wires, I_s increases between 50% for Nb-33%Zr and 75% for Nb-25%Zr over identical, unplated wire coils. I_s of solenoids wound with plated, unstable wires (C-101, C-102, and C-103) increases less than 25%. Conversely, unplated wires carry approximately the same solenoid current regardless of super-current stability; i.e. coil C-104 (unstable wire) and coil C-107 (stable wire) carried essentially the same I_s.

It is important to note the correspondence between the unstable region and solenoid critical currents. Generally, if the solenoid load line (H/I = constant) enters the unstable region, the solenoid will go normal. Copper plating allows greater penetration into the unstable region, and the extent of penetration increases with the stability of the wire.

The variations in super-current stability of these wires are attributed to different metallurgical structures arising from dissimilar manufacturing processes. Not only do the stabilities vary between the suppliers but also have improved during the course of these investigations. For example, the two wires from Supplier B, Figures 7 and 11, as well as the two from Supplier C, Figures 8 and 9, exhibit different degrees of stability. In both cases, the more stable wires are of more recent manufacture.

D. METALLURGICAL EXAMINATIONS

Metallurgical examinations of the above wires reveal no systematic structural variations which can be correlated with super-current stability. The X-ray diffraction data* show that all wires, except the Nb-25%Zr from Supplier A, are

---

* Second phases must be present in amounts $\geq$ 5% to be seen in diffraction patterns.

entirely β-Nb (cubic) phase. The wire from Supplier A has a small percentage of hexagomal α - Zr and excess Nb.

The representative photomicrographs in Figure 12 exhibit small amounts of cold-work-stringered, second-phase precipitate, except for the Supplier A wire. Specifically, there is no difference between the photomicrographs of the Supplier C (unstable), Supplier B (unstable) and Supplier B (stable) wires. The Supplier D photomicrograph shows essentially the same structure except that the precipitate size is smaller. The second phase is probably α - Zr or the accompanying β - Nb^2 and could result from heat treatment or from O_2 or N_2 content.

The photomicrograph of the Supplier A, Nb-25%Zr wire (unstable) shows a heavily striated structure with no obvious second-phase precipitate although α - Zr was seen in the X-ray diffraction patterns. Since the photomicrograph and X-ray results indicate that this wire has a different metallurgical structure, one might expect a significant difference in stability. However, the short-sample and magnet behavior is the same as for other unstable wires.

It is apparent from the above discussion that post-cold-work metallurgical examinations are of little value in predicting super-current stability.

IV. WIRE DIAMETER EFFECTS

The effect of wire diameter on short sample and solenoid critical currents has been investigated for Nb-33%Zr. Copper-plated and unplated wires of 0.013, 0.025, 0.051, and 0.076 cm dia were drawn from one ignot and were subject to the same metallurgical and drawing processes. Chemical analyses confirmed that all wires were the same alloy. Post-cold-work X-ray diffraction patterns and photomicrographs reveal no metallurgical differences although discussions in the preceeding section indicate that these two tests are not very significant.

Short samples and solenoids of each wire were tested. Pertinent solenoid data is listed in Table 3. Coil construction parameters such as geometry, wire length, and spacing between turns and layers vary ± 10% except for coils C-D1 and C-D2. The space factors for these two coils are 30% less than the average because the insulation and plating occupy proportionately more volume as wire diameter decreases. For coils C-D5 through C-D8, filler was used to maintain consistent spacing.

Short sample critical current density, J_c, <u>versus</u> applied field and solenoid critical current density, J_s, <u>versus</u> generated field are shown in Figure 13. Figure 14 shows J_c (at 25 kG) and J_s as functions of wire diameter for plated and unplated wires. In all cases, J_c and J_s decrease with increasing diameter and increase for copper-plated wires.

Current degradation is taken as the ratio of J_s to J_c, where J_c is the inter-cept of the J_c-H curve and the solenoid load line (H = const. x J). This ratio is plotted as a function of wire diameter in Figure 15 for plated and unplated wires. Degradation increases with wire diameter and is greater for unplated wire.

The most efficient wire diameter is that which gives the highest effective solenoid current density, $J_s \lambda$, where J_s is found from Figure 15 and λ is the packing factor. As mentioned above, λ decreases with wire diameter. For copper-plated wire and practical solenoid construction techniques, $J_s \lambda$ has a

broad maximum between the diameters of 0.013 and 0.025 cm. If the cost of the wire is considered, the 0.025 cm dia wire is the most economical.

V. SN TRANSITIONS IN SOLENOIDS

A multi-probe solenoid has been constructed to investigate the origin of SN transitions. This coil is wound with 0.025 cm dia Nb-33%Zr wire, potted in Stycast 2850-FT epoxy, and instrumented with 85 pairs of voltage probes. The coil parameters are a_1 = 1.27 cm, α = 2.3, β = 2.99, H/I = 1.01 kG/A, and L = 0.7 henry.

Each probe-pair monitors one cm of the Nb-Zr wire. The number and location of the pairs are such that at least one pair must be in the transition region. The probes are individually monitored with an array of magnetic cores. If a probe is in the normal region, the resistive voltage across the probe reverses the magnetization of the magnetic core. The resistive voltage across a probe is more than an order of magnitude greater than the opposing inductive voltage. After a transition all cores are checked for reversal, and the normal region is mapped.

The magnet was driven normal by increasing the current at a rate of 44 mA/sec. Three separate runs and a total of twelve transitions were made. The solenoid was warmed to room temperature between runs so that the training cycle could be repeated.

Two important results were obtained from this experiment. First, the transition <u>always</u> originates at the axial center of the inner windings - the highest field region. Typical results are illustrated in Figures 16 and 17. Figure 16 shows the time dependent behavior of solenoid current, resistance, and voltage during an SN transition. Figure 17 is a cross-sectional view of the solenoid and shows the location and shape of the normal region as determined from the voltage probes for the transition depicted in Figure 16. The region outlined in Figure 17 accounts for 65% of the magnetic energy. The remaining energy is not recorded due to lack of sensitivity of the sensing array.

The fact that the transition initiates in the highest field region of the multi-probe coil does not mean that transitions in high field coils ($>$ 30 kG) will also

initiate at this location. The 17.1 kG of the multi-probe solenoid is in the edge of the unstable region discussed in Section III. If the central field were higher than the upper limit on the unstable region (> 30 kG) it is possible that the transition would initiate in the region of unstable field, which would be in the interior region of the solenoid.

The second result is that joule heating is not the predominant means of propagating the normal region. In particular, the 6 cm axial dimension of the normal region in Figure 17 is far too large to have grown solely due to thermal propagation. In the thermal model the axial length is $\int_0^{t_m} V_z \, dt$, where V_z is the propagation velocity perpendicular to the wire in the axial direction and t_m is the practical duration of the transition. V_z is related to V_θ, the propagation velocity along the wire, through thermal properties of the solenoid and $V_z \leq 0.3 V_\theta$. Since the dependence of V_θ on current and field is reported,[3,4] the integral can be estimated and is found to be less than 0.2 cm. This dimension is considerably less than the actual length of 3 cm measured from the axial center of the coil. In addition, since the radial thermal velocity, V_r, is approximately equal to V_z for our test solenoid, the shape of the normal region would approach a semicircle if thermal propagation were dominant instead of the oblong shape shown in Figure 17.

From the above results, it is evident that joule heating is not the principal mechanism for propagating the normal region, and some other means must predominate.

17

VI. THERMAL AND MECHANICAL PARAMETERS

The effect of thermal environment and mechanical constraint on I_s has been investigated by potting small solenoids in epoxies which have different thermal conduction and expansion coefficients. Five small solenoids were constructed with the following parameters: a_1 = 0.63 cm, α = 2, β = 2, wire length = 80 m, and H/I = 513 gauss/A. The solenoids were wound from a 600 m piece of unplated, fused-nylon insulated, 0.025 cm dia Nb-33%Zr wire. The coils were impregnated during winding with the epoxies listed in Table 4. The epoxy fillers were varied to change the thermal expansion and conduction coefficients. Solenoid critical currents are listed in Table 5 with the appropriate potting compound. The variations in critical current are too small to draw any definite conclusions as to the effect of the various environments, although trends do appear. The critical currents increased with the thermal conductivity of the epoxies; and, for the coils with similar thermal expansion coefficients, L-1 and L-4, the coil with greater thermal conductivity carried more current. Although these results are not conclusive, it appears that the thermal environment of a solenoid effects I_s only slightly.

The role of mechanical constraint cannot be isolated in the above tests, but I_s for the plated-wire coils listed in Table VI did not vary significantly due to potting in the Emerson and Cuming Stycast 2850 FT epoxy.*

A surprising and unexplained result should be mentioned. Coil C-110, wound with Nb-33%Zr wire and potted in Stycast 2850 FT,* carried an unusually high current of 32A and generated 37 kG. This result could not be duplicated with subsequent, similarly constructed solenoids.

---

* This epoxy has a small diamagnetic moment which does not affect the critical current.

VII. SUMMARY

Various aspects of the current degradation phenomenon in Nb-Zr wires have been studied and reported above. The results are briefly summarized below.

1. The critical current, I_s, for <u>unplated</u> Nb-25%Zr wire solenoids has been correlated with the number of layers of a solenoid and spacing between wires as shown in Figures 3 and 4. These graphs can be used to predict I_s to better than ± 10% for the above wire, but only qualitative extrapolations can be made to other alloy systems.

2. The critical current for <u>copper-plated</u> wire solenoids obeys Equation 2 in the text. The constants in the equation are empirically determined as shown in Figure 5. These results predict I_s to ± 5% and appear to be universal for 0.025 cm dia Nb-Zr wire.

3. Critical current densities of short samples and solenoids, for plated and unplated wires, increase with decreasing diameter as shown in Figures 13 and 14. Current degradation also decreases with increasing diameter as shown in Figure 15. The effect of copper-plating, evident in all relevant figures, is to increase the critical current in short samples and solenoids while reducing degradation.

4. Mechanical and thermal effects on solenoid currents are found to be small, although I_s increases slightly with an increase in the thermal conductivity of the solenoid potting material. Mechanical constraint does not obviously increase I_s once the wires are reasonably secured.

5. The SN transition study shows that the normal region is always initiated at the same location which, for our solenoid, is the highest field region; i.e. at the inner windings on the median plane. Furthermore, the normal region propagates predominately by some mechanism other than joule heating.

6. The various methods of testing short samples show that super-current instabilities can be caused by time varying magnetic fields. Attempts to correlate these instabilities with metallurgical history were unsuccessful and

demonstrate that post-cold-work metallurgical examinations of commercially prepared wires are essentially unrevealing.

The results of the investigations of geometrical parameters, wire diameter, and mechanical and thermal properties are useful in the design of superconducting solenoids, but indicate that these effects are only contributors and are not basic to the degradation problem. Conversely, the studies of SN transitions, short-wire current instabilities, and metallurgical parameters are essential to the understanding of degradation and should be pursued further.

REFERENCES

1. Rosner, C. H., M. G. Benz, and D. L. Martin, J. Appl. Phys. 34, 7, p. 2107. July, 1963

2. Rogers, B. A., D. F. Atkins, Trans. A.I.M.E. 203 (1955) 1034

3. Whetstone, C. N., A. D. McInturff, D. B. Sullivan, and C. E. Roos, Bull. Amer. Phys. Soc., 7, 523, 1962;

    Whetstone, C. N. and C. R. Sullivan, Bull. Amer. Phys. Soc., 8, 557, 1963;

    Whetstone, C. N. and C. E. Roos, Bull. Amer. Phys. Soc., 9, 455, 1964;

    Whetstone, C. N., "Thermal Phase Transitions in Superconducting Nb-Zr Alloys," Ph.D. Thesis, Vanderbilt University, 1964

4. Stekly, Z. J. J., "Theoretical and Experimental Study of an Unprotected Superconducting Coil," International Cryogenic Engineering Conference, UCLA, 1962

TABLE I

SOLENOID CONSTRUCTION AND OPERATING DATA* FOR THE GEOMETRICAL INVESTIGATIONS

Coil	a_1 (cm)	α	β	N (turns)	N_r (layers)	Wire Length (m)	$H(I_s)$ (kG)	I_s (A)
1	0.63	1.02	2.00	91	1	7.3	2.8	71
2	0.63	1.05	2.00	182	2	14.8	4.5	56
3	0.63	1.08	2.00	273	3	22.9	5.1	43
4	0.63	1.10	2.00	364	4	30.5	5.8	37
5	0.63	1.13	2.00	455	5	39.0	6.9	35
6	0.63	1.18	2.00	637	7	55.5	8.1	30
7	0.63	1.26	2.00	910	10	83.2	10.2	27
8	0.80	2.81	4.76	10086	41	965	27.6	15.0
9	0.80	3.66	4.66	16000	60	1770	35.4	15.2
10	0.96	1.86	3.98	5738	24	488	15.5	17.4
11	3.43	1.17	2.70	10082	18	2590	12.8	19.2
12	0.80	2.33	5.31	7900	32	410	19.3	17.2
13	0.80	3.01	5.28	12446	48	3790	28.9	16.8
14	0.80	4.43	5.31	21511	82	6550	44.5	16.3
15	0.80	4.72	5.40	24623	84	7500	42.3	13.4
16	0.63	3.80	2.04	3332	52	320	20.7	19.2
17	0.80	4.68	5.32	13655	88	1950	33.3	18.8
18	0.80	4.62	5.40	17900	84	2540	36.4	15.8
19	0.80	3.70	5.23	6372	40	746	18.1	21.0
20	3.46	1.23	2.53	14056	23	3400	16.7	18.0

* For 0.025 cm dia, unplated Nb-25%Zr wire

TABLE II

SOLENOID DATA FOR Nb-Zr WIRES OF DIFFERENT STABILITIES

Solenoid	Alloy (%Zr)	Stability	Supplier	Copper Plated	a_1 (cm)	α	β	H/I (kG/A)	I_s (A)	H_s (kG)
C-101	25%	unstable	A	Yes	1.16	2.50	2.20	1.16	25.9	30.0
C-103	25%	unstable	B	Yes	1.15	2.5	2.2	1.2	17.5	21.0
C-104	25%	unstable	C	No	0.80	2.34	3.00	1.12	17.2	19.3
C-105	25%	semi-stable	C	Yes	1.14	2.51	2.21	1.16	32.0	37.0
C-108	25%	semi-stable	D	yes	1.15	2.40	2.20	1.12	35.5	39.8
C-102	33%	unstable	A	Yes	1.15	2.50	2.20	1.16	22.2	25.8
C-106	33%	stable	B	Yes	1.14	2.57	2.23	1.14	25.8	29.4
C-107	33%	stable	B	No	1.14	2.58	2.24	1.13	17.8	20.3
C-109	33%	semi-stable	D	Yes	1.15	2.62	2.22	1.24	28.0	34.7

TABLE III

SOLENOID DATA FOR VARIOUS DIAMETER Nb-33%Zr WIRES*

Solenoid	Wire Dia. (cm)	Copper Plate Thickness, Radius (cm)	Wire Weight (kG)	α	β	H/J $\dfrac{\text{gauss cm}^2}{A}$	J_s (10^4 A/cm^2)	H_s (kG)
C-D1	0.013	None	0.27	2.90	2.19	0.44	4.42	19
C-D2	0.013	0.0025	0.28	2.73	2.19	0.48	8.85	43
C-D3	0.025	None	0.32	2.70	2.2	0.56	3.86	22
C-D4	0.025	0.0025	0.32	2.56	2.20	0.58	5.82	34
C-D5	0.051	None	0.28	2.53	2.2	0.52	1.50	7.8
C-D6	0.051	0.0051	0.30	2.47	2.20	0.59	3.82	22
C-D7	0.076	None	0.31	2.50	2.18	0.60	1.32	7.9
C-D8	0.076	0.0076	0.32	2.46	2.22	0.61	2.26	13.9

* All coils are wound with Supplier D, Nb-33%Zr wire on 2.3 cm ID spools

TABLE IV

EPOXY POTTING COMPOUNDS USED IN THE THERMAL EFFECT SOLENOID

Coil	Epoxy and Filler
L-1	Emerson and Cuming Stycast 2850 FT is an alumina filled epoxy and has a thermal expansion coefficient equal to that of copper at room temperature. The alumina results in a high heat transfer coefficient at 4.2°K.
L-2	Hysol #2038 plus #3475 is a typical epoxy with high expansion coefficient and low thermal conductivity.
L-3	This epoxy is the same as in L-2 above, but is filled with alumina. Less alumina than in the Stycast 2850 FT was used to provide a thermal conductivity between the conductivities of the 2850 FT and the Hysol.
L-4	Emerson and Cuming Stycast-1090 is filled with hollow spheres of boron silicate. The thermal expansion coefficient is the same as 2850 FT, but the thermal conductivity is reduced by an order of magnitude at room temperature.
L-5	No epoxy. Mylar sheet, 0.005 thick was used to provide the required space factor.

TABLE V

CRITICAL CURRENTS OF THERMAL EFFECT SOLENOIDS*

Coil	Epoxy	I_s (A)
L-1	Stycast 2850 FT	31.0
L-3	Hysol with Alumina	30.3
L-2	Hysol	29.2
L-4	Stycast 1090	29.2
L-5	No Epoxy	27.9

* All solenoids used 0.025 cm dia Nb-25% Zr wire.

TABLE VI

COMPARISON OF EPOXY POTTED* AND UNPOTTED SOLENOIDS**

Solenoid	Epoxy	Copper Plated	a_1 (cm)	α	β	H/I (kG/A)	I_s (A)	H_s (kG)
C-107	No	No	1.14	2.58	2.24	1.13	17.8	20.3
C-110	Yes	No	1.15	2.46	2.18	1.16	32.3	37.5
C-111	No	Yes	1.15	2.49	2.23	1.14	27.4	31.2
C-106	Yes	Yes	1.14	2.57	2.23	1.14	25.8	29.4

* Emerson and Cuming 2850 FT

** All coils use 0.025 cm dia Nb-33%Zr Wire

27

I_c (H = 0) = 180A

UNPLATED 0.025 cm dia
Nb−25 % Zr WIRE, 4.2 °K

TYPICAL SHORT SAMPLE CRITICAL CURRENTS, I_c

SOLENOID CURRENTS, I_s, LIE IN THIS AREA

I (A)

H (kilogauss)
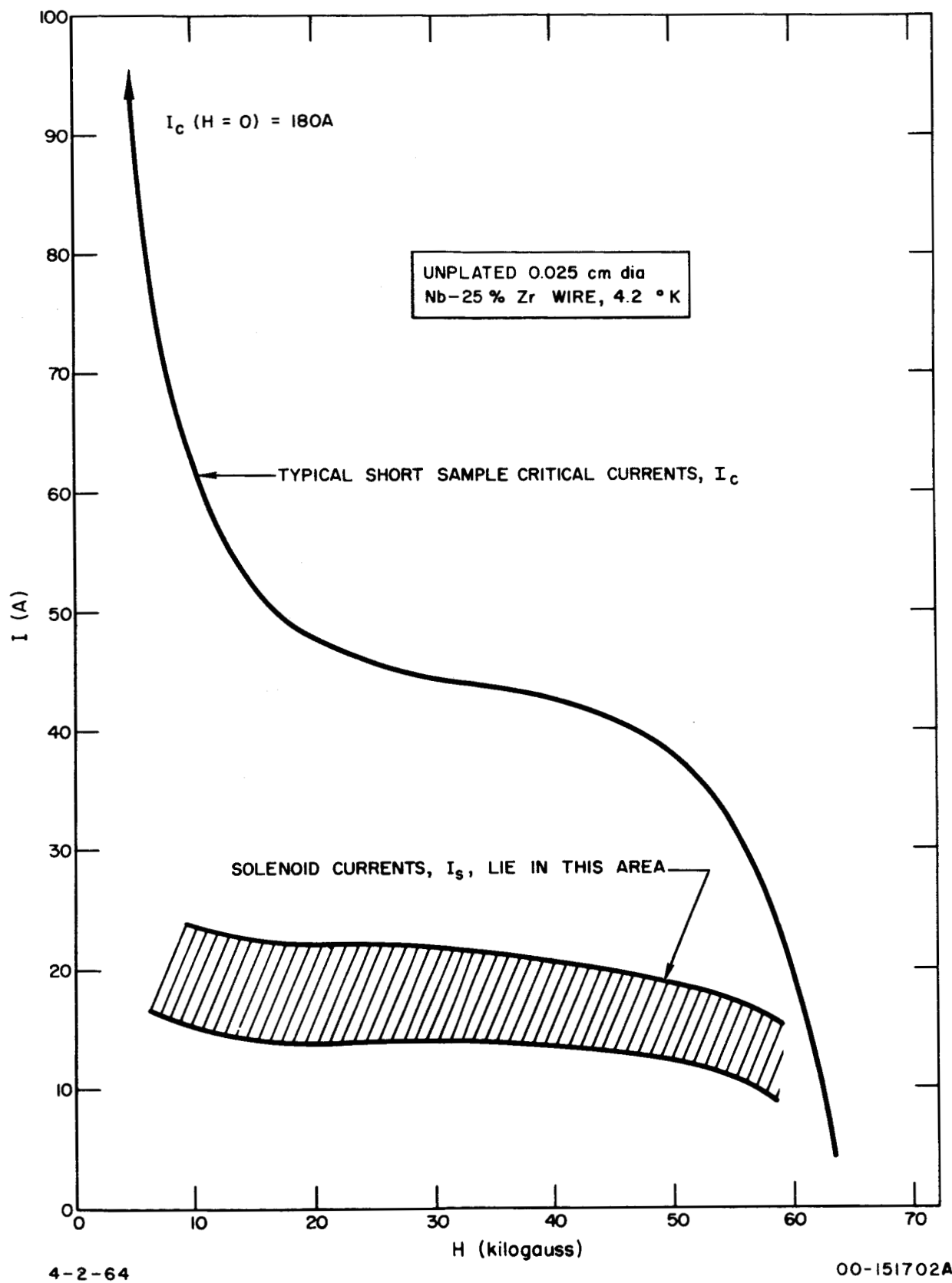
4-2-64

00-151702A

Figure 1. Typical Critical Currents for Short Samples and Solenoids

28
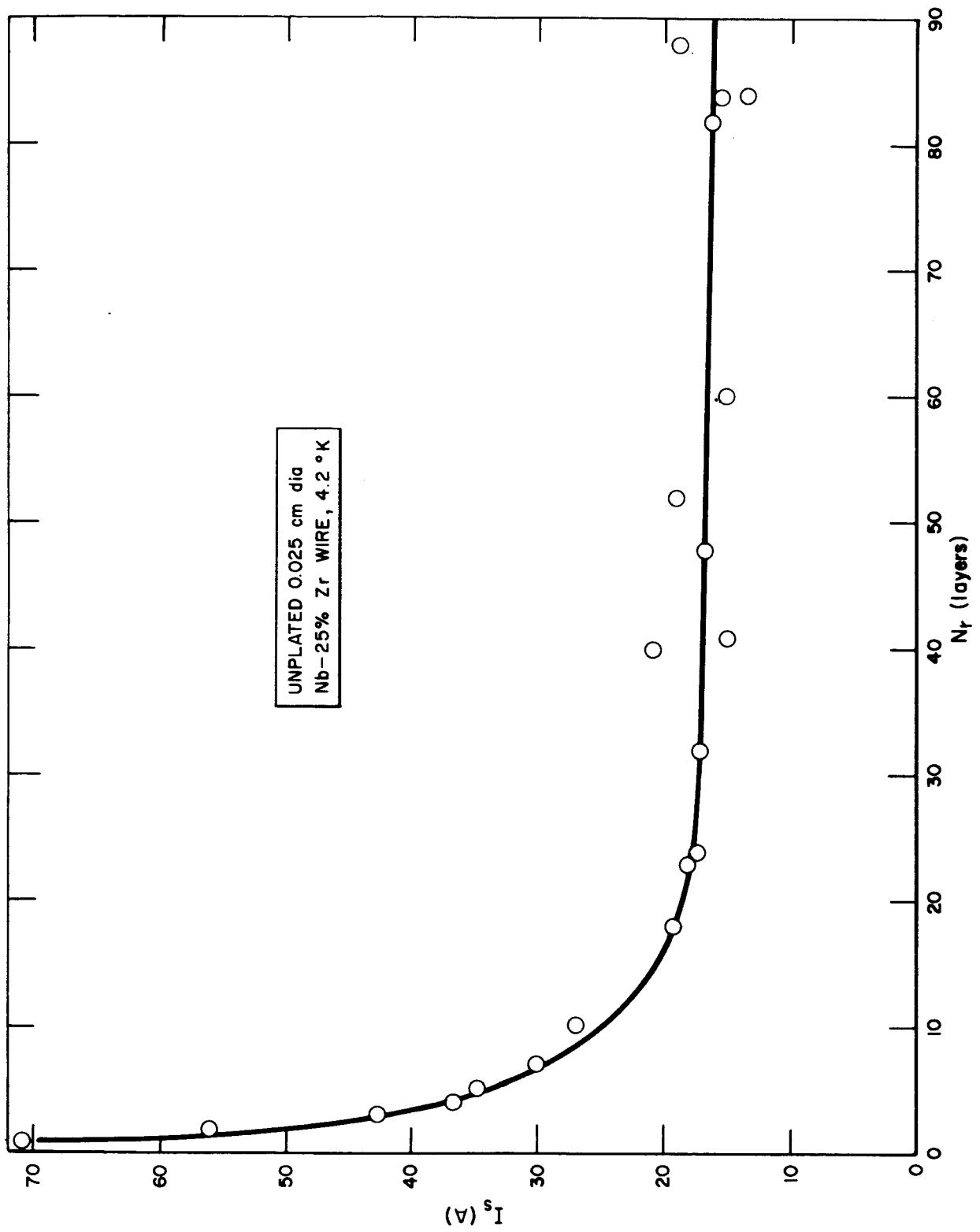
Figure 2. Solenoid Critical Current versus Number of Winding Layers

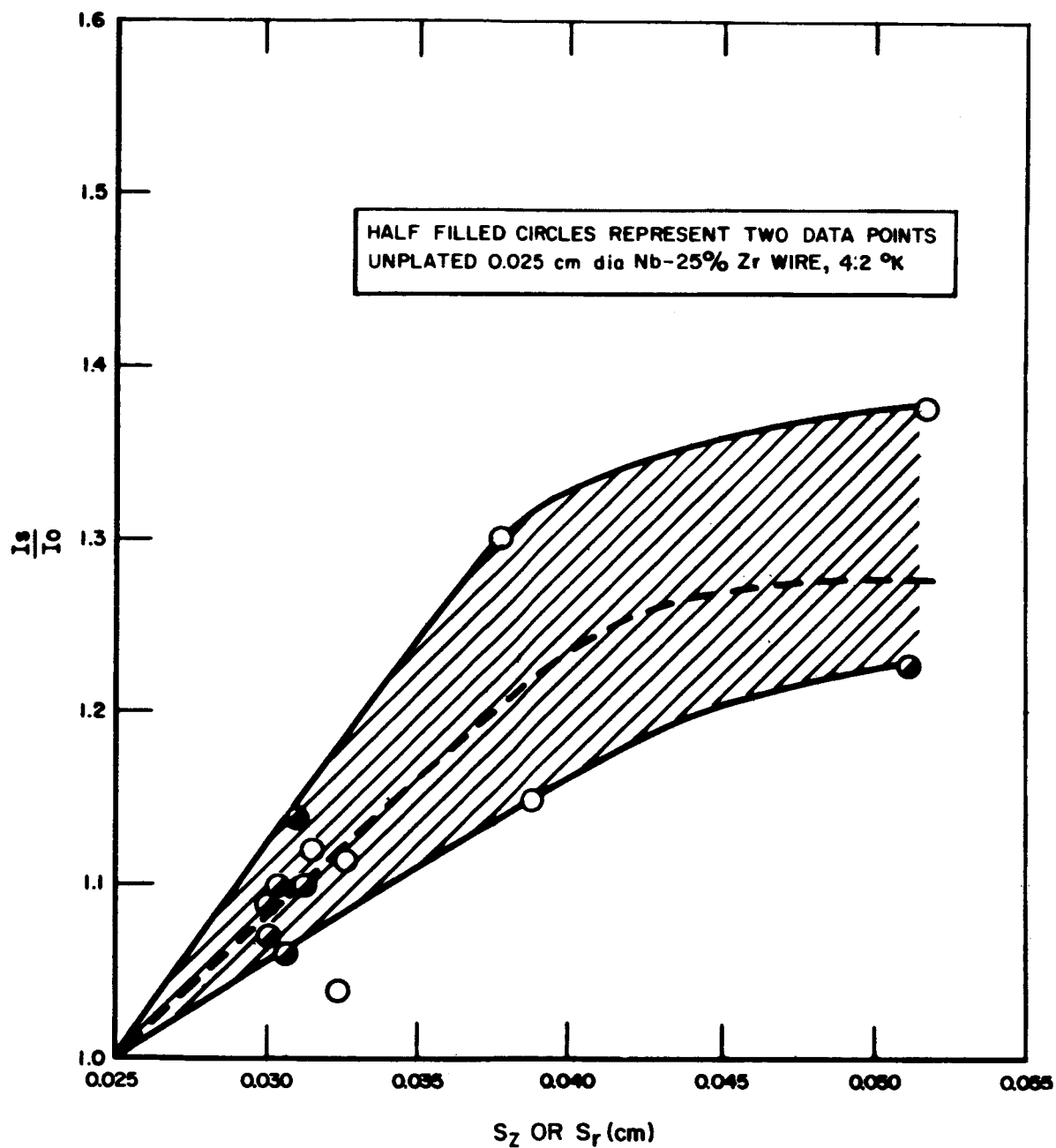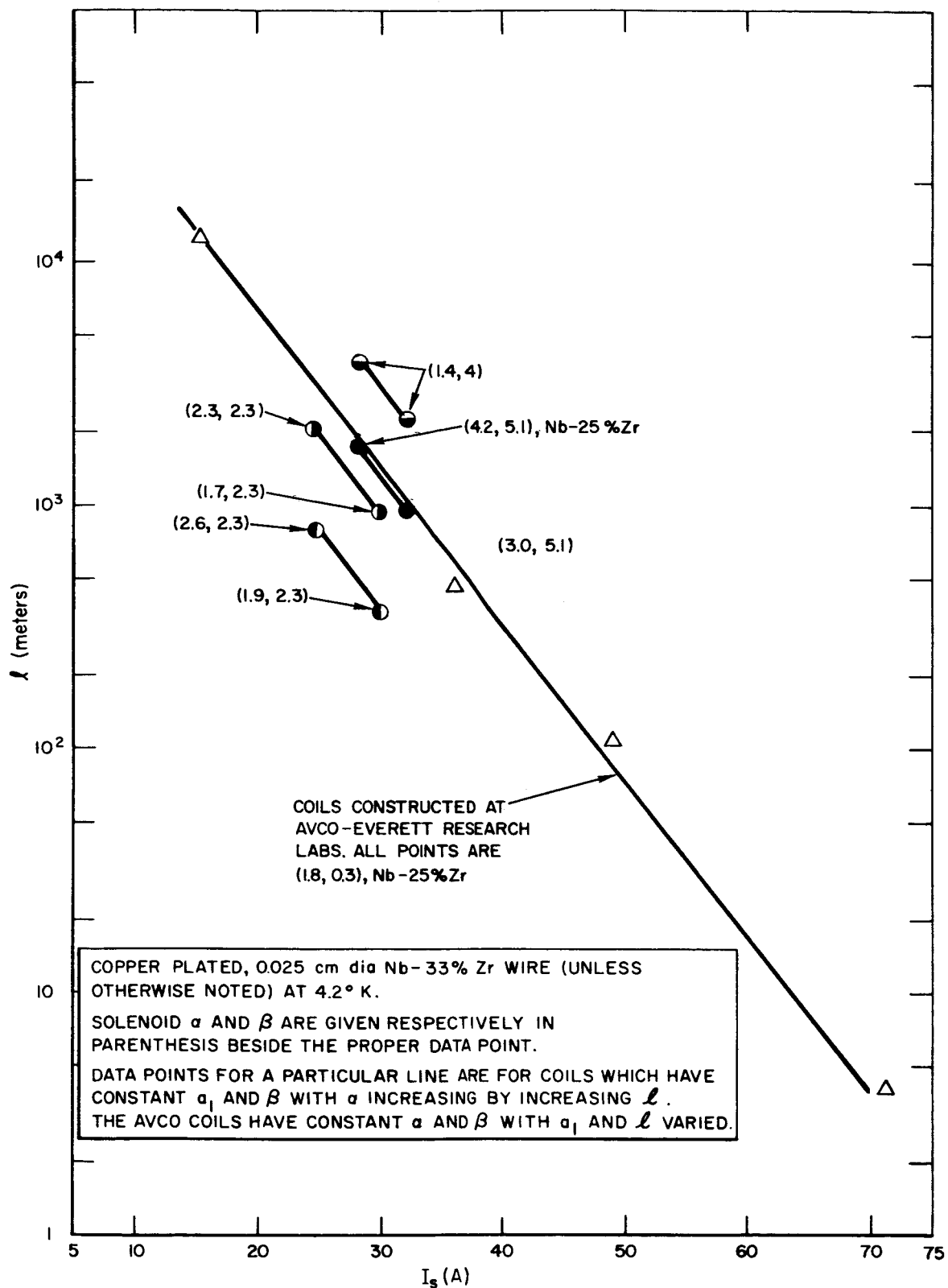OO-I5I703A

4-2-64

29
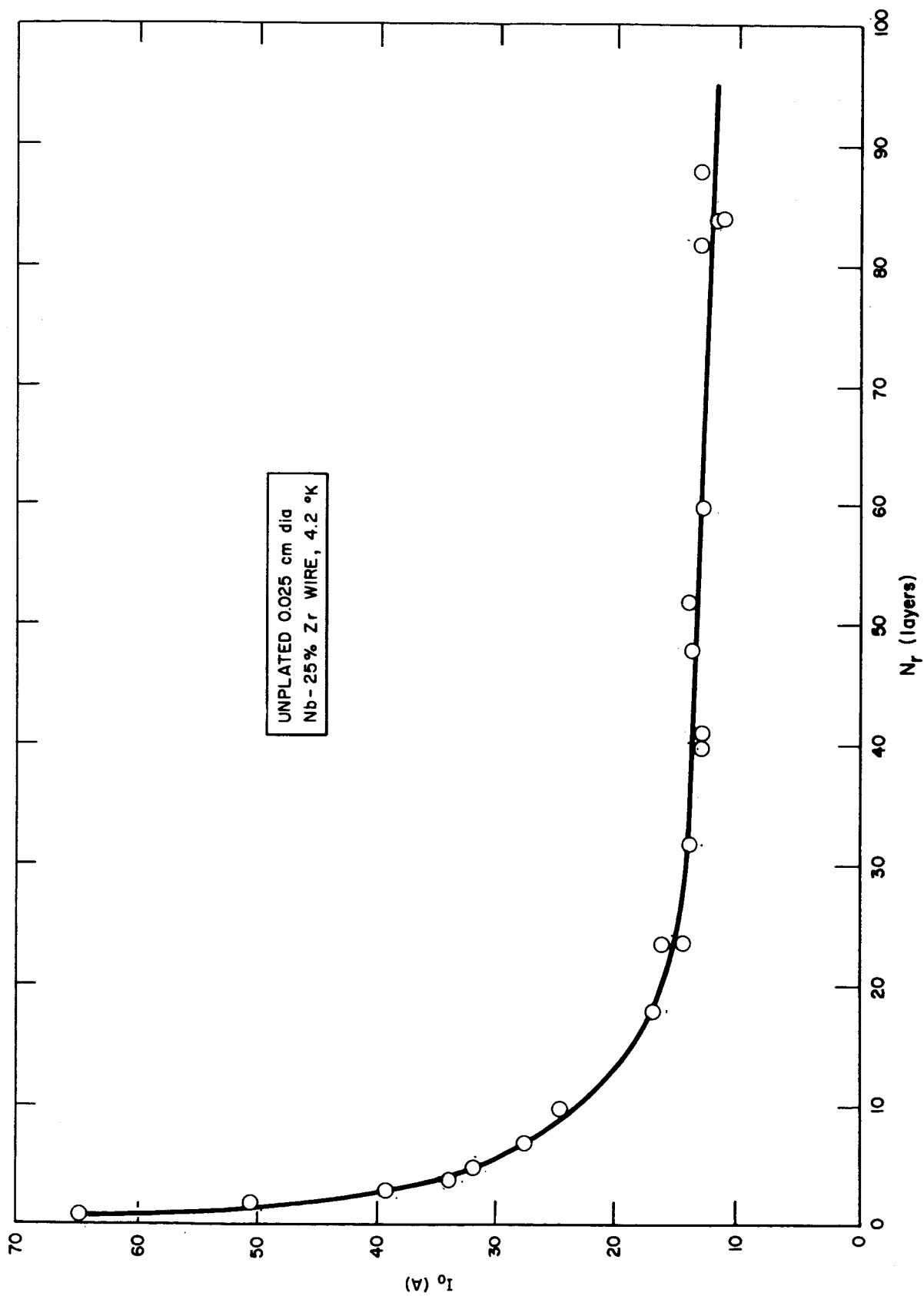
Figure 3. Solenoid Critical Currents as a Function of Wire Spacing
(Solenoid Currents are Normalized to the Current for Touching Bare Wires)

00-151704A

4-2-64

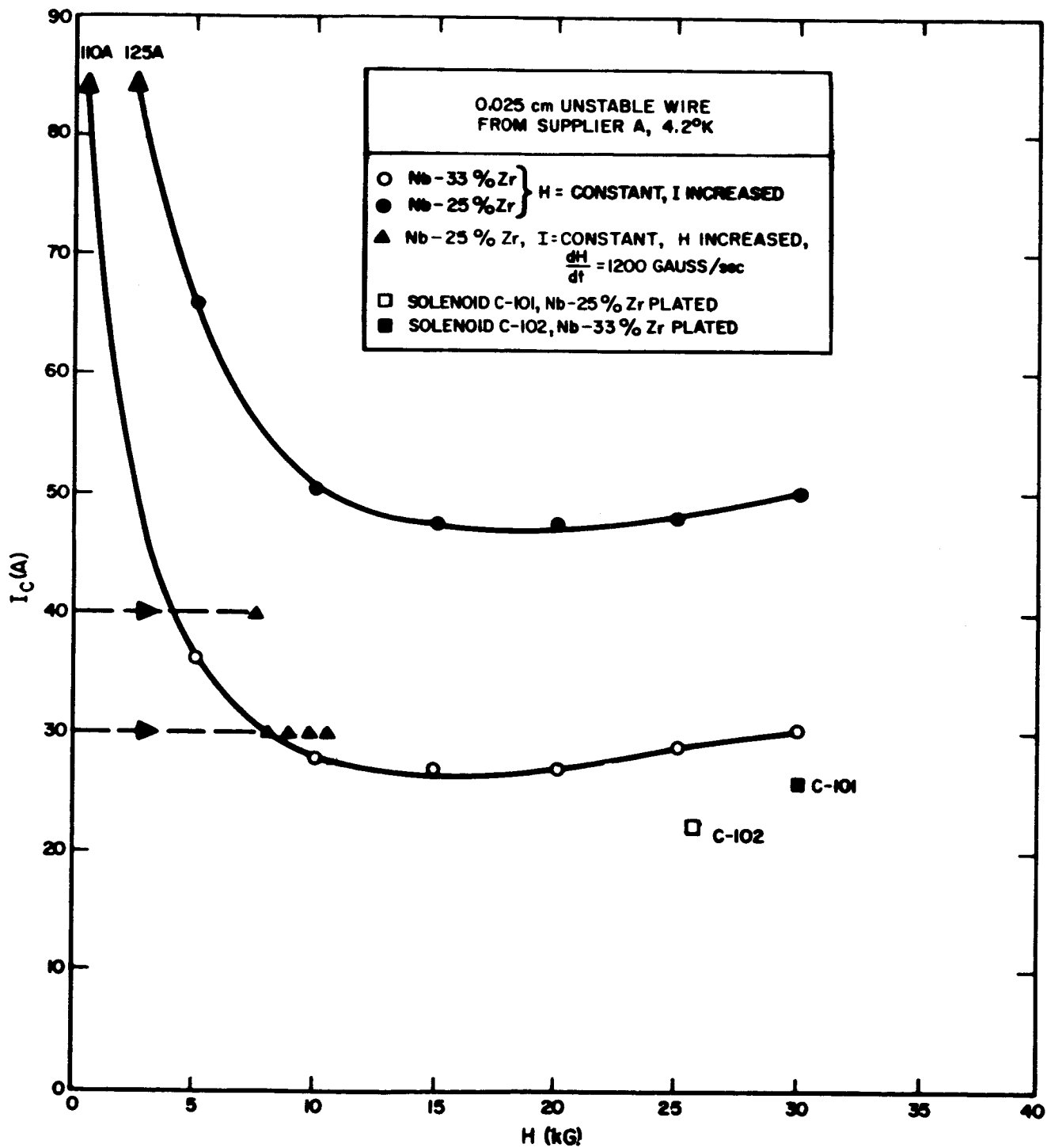30

HALF FILLED CIRCLES REPRESENT TWO DATA POINTS
UNPLATED 0.025 cm dia Nb-25% Zr WIRE, 4:2 °K

00-151705® 18

Figure 4.   Extrapolated Solenoid Current for Touching Uninsulated Wires
versus Number of Winding Layers

The chart contains the following labels and text:

- 10^4
- 10^3
- 10^2
- 10
- 1
- (1.4, 4)
- (2.3, 2.3)
- (4.2, 5.1), Nb-25 %Zr
- (1.7, 2.3)
- (2.6, 2.3)
- (3.0, 5.1)
- (1.9, 2.3)
- COILS CONSTRUCTED AT AVCO-EVERETT RESEARCH LABS. ALL POINTS ARE (1.8, 0.3), Nb-25%Zr
- ℓ (meters)
- I_s(A)
- 5 10 20 30 40 50 60 70 75

COPPER PLATED, 0.025 cm dia Nb-33% Zr WIRE (UNLESS OTHERWISE NOTED) AT 4.2° K.

SOLENOID α AND β ARE GIVEN RESPECTIVELY IN PARENTHESIS BESIDE THE PROPER DATA POINT.

DATA POINTS FOR A PARTICULAR LINE ARE FOR COILS WHICH HAVE CONSTANT α_1 AND β WITH α INCREASING BY INCREASING ℓ. THE AVCO COILS HAVE CONSTANT α AND β WITH α_1 AND ℓ VARIED.

4-2-64

00-151706C

Figure 5. Wire Length versus Solenoid Critical Current for Copper-plated Wire

32

Figure 6. Critical Currents for Short Sample Tests and Solenoids:
Type A Wire
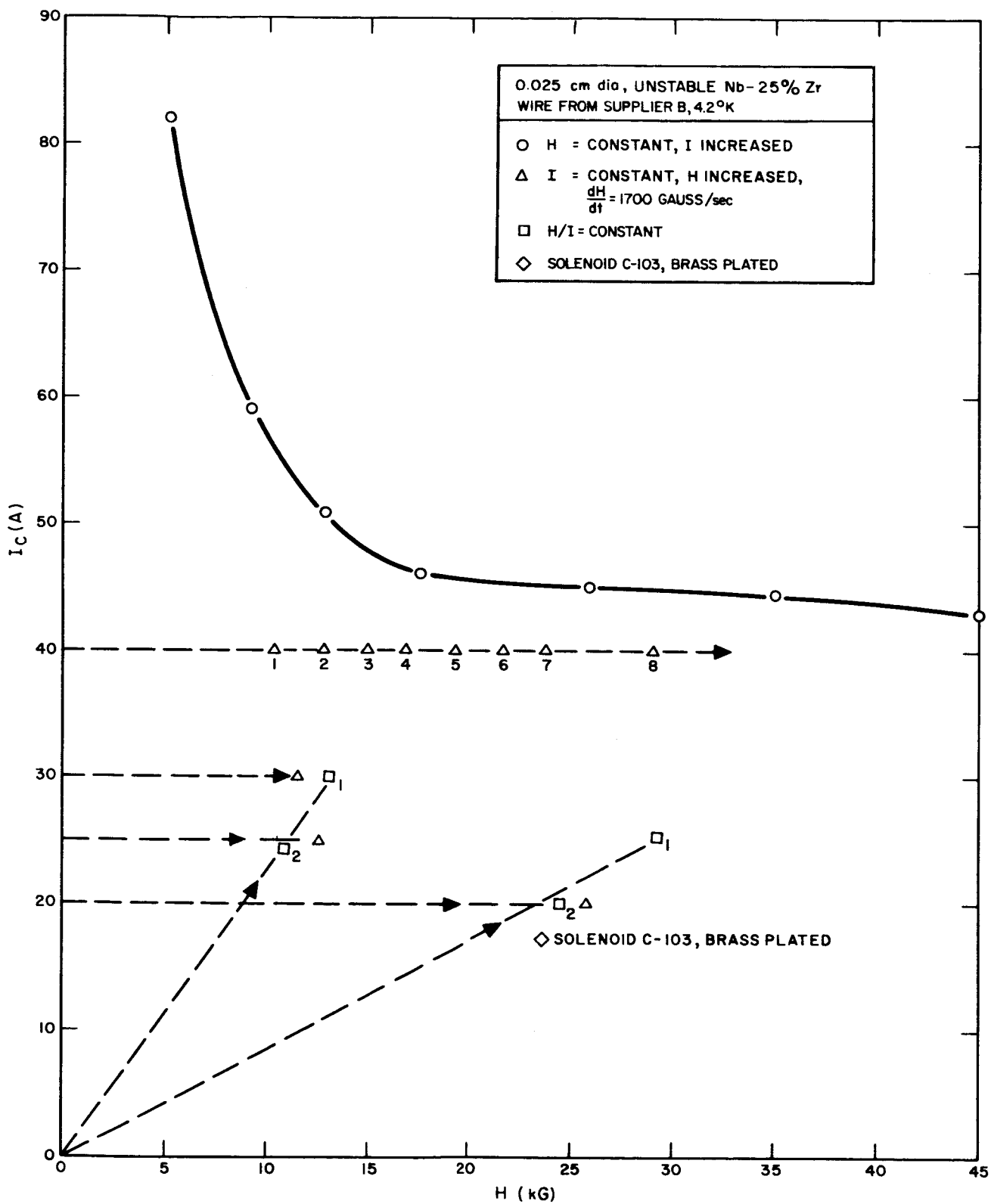
Figure 7. Critical Currents for Short Sample Tests and Solenoids:
Unstable Type B Wire

90

80

70

$I_C(A)$

60

50

40

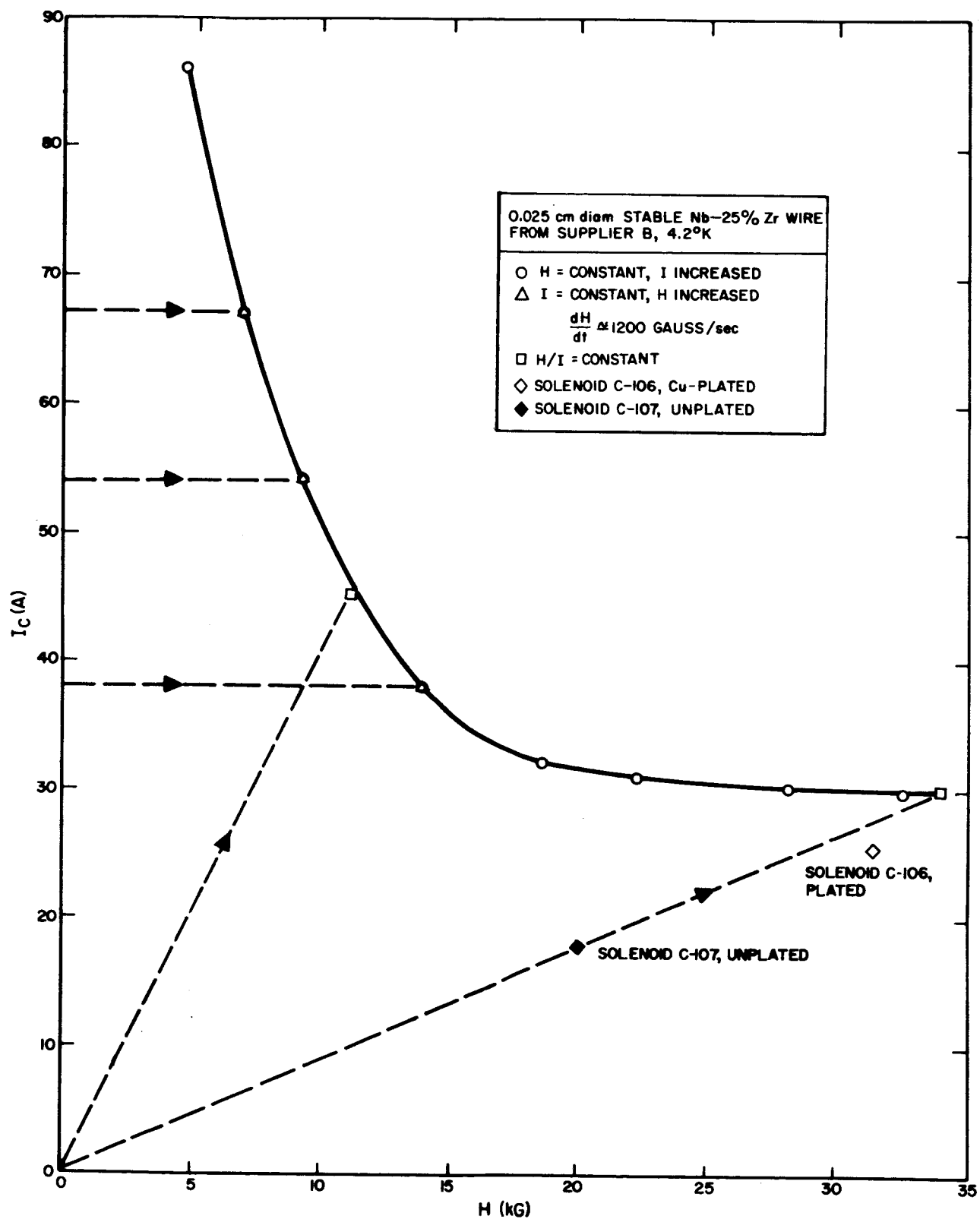30

20

10

0

0.025 cm dia Nb-25% Zr UNSTABLE
WIRE FROM SUPPLIER C, 4.2°K
OPEN AND CLOSED POINTS ARE
FOR DIFFERENT SAMPLES

O H = CONSTANT, I INCREASED
△ I = CONSTANT, H INCREASED,
   $\frac{dH}{dt} \simeq$ 1200 GAUSS/sec

□ H/I = CONSTANT
◇ SOLENOID C-104, UNPLATED

SOLENOID C-104, UNPLATED

0   5   10   15   20   25   30   36

H (kG)
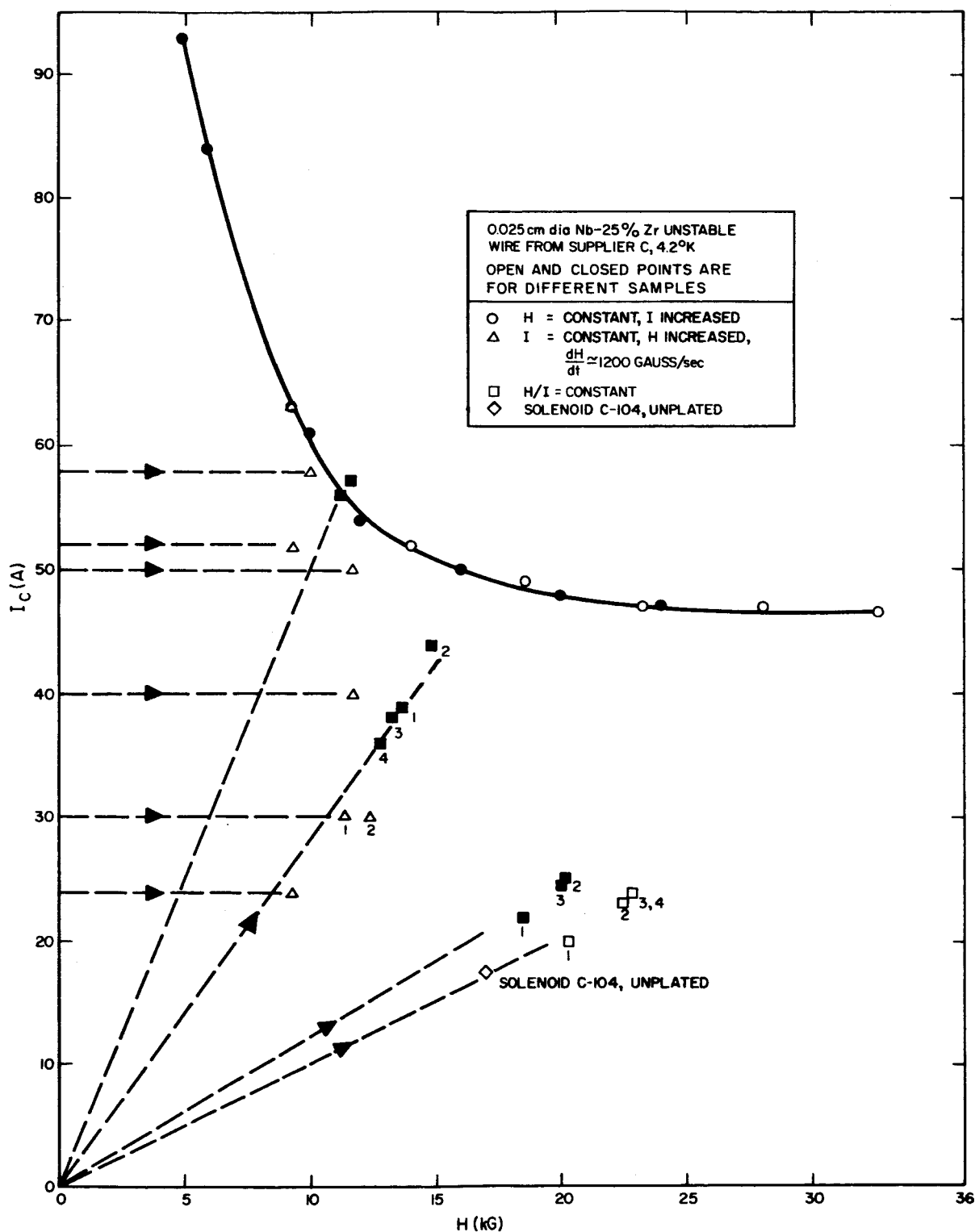
9-16-64   2468-1501

Figure 8. Critical Currents for Short Sample Tests and Solenoids:
Unstable Type C Wire

35
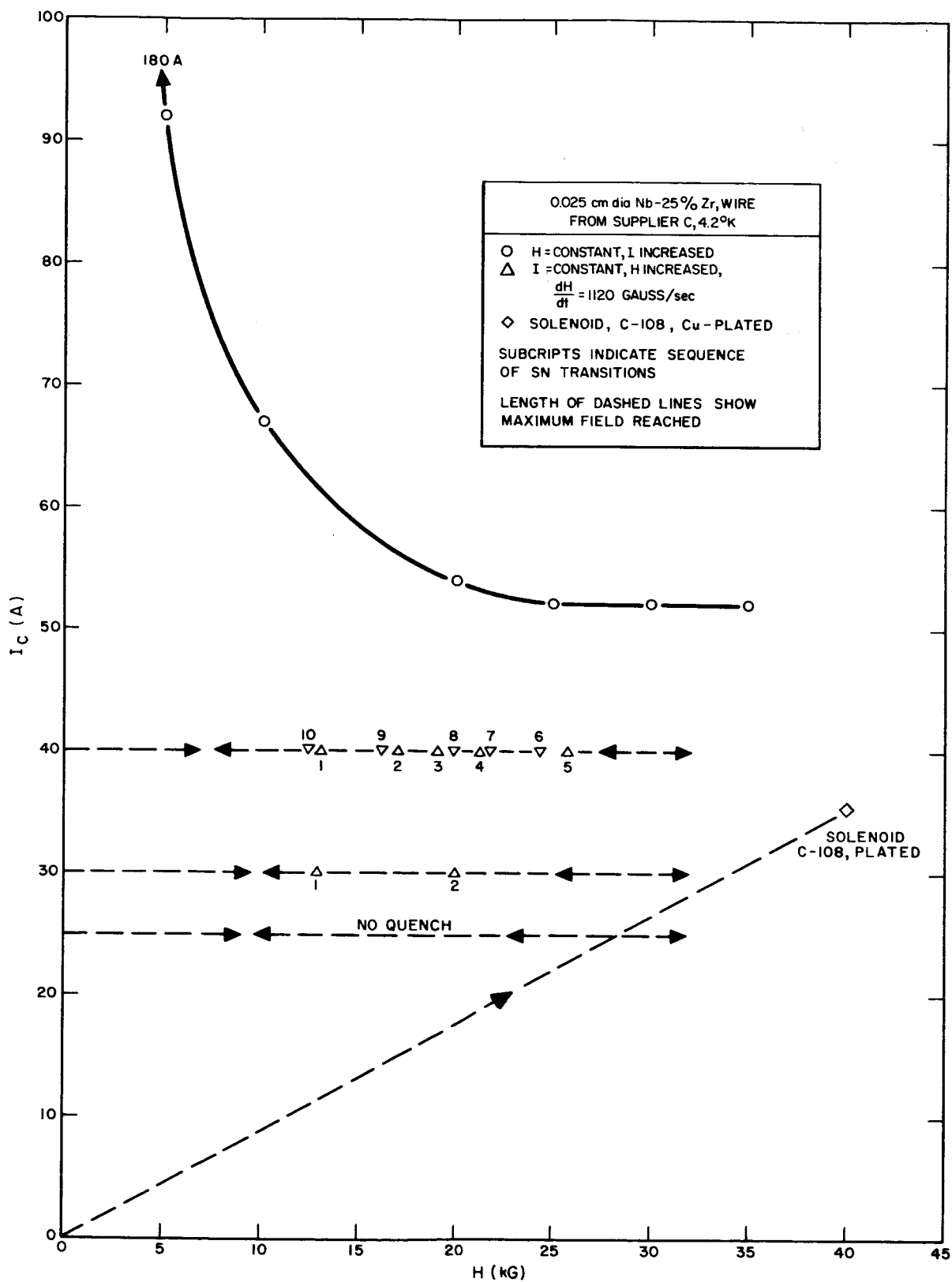
Figure 9. Critical Currents for Short Sample Tests and Solenoids:
Semi-stable Type C Wire
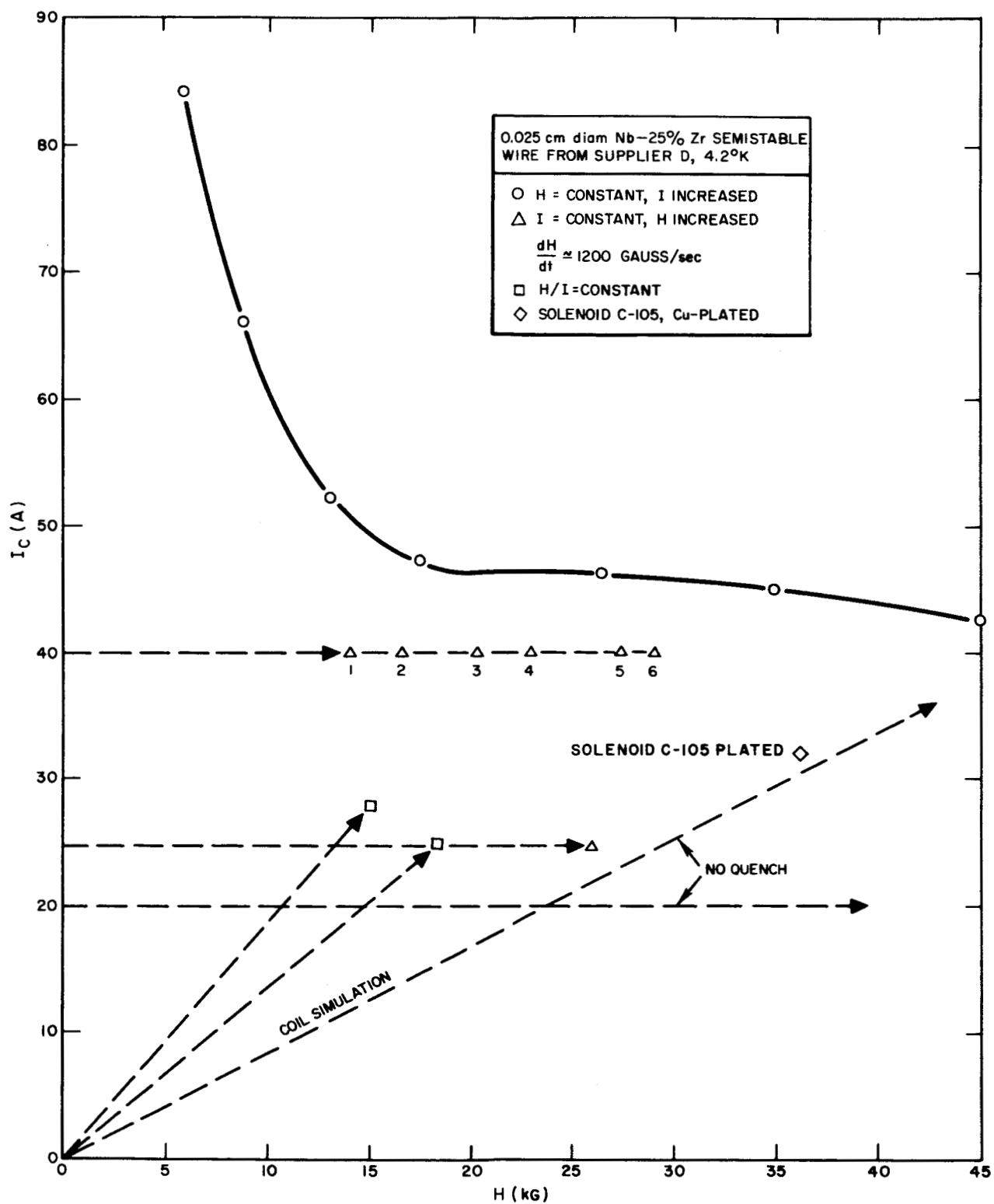
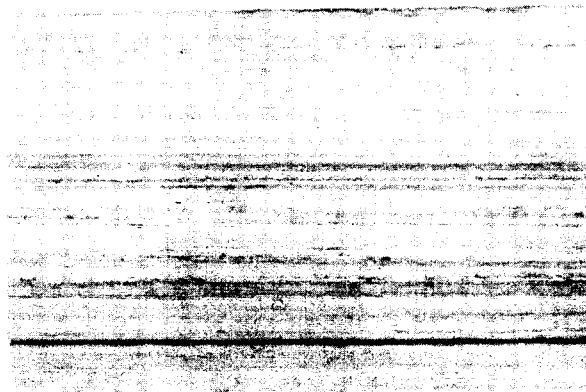Figure 10. Critical Currents for Short Sample Tests and Solenoids: Semi-stable Type D Wire

9-16-64

2468-1507

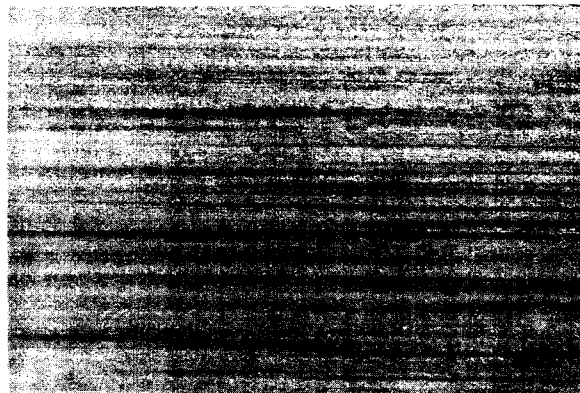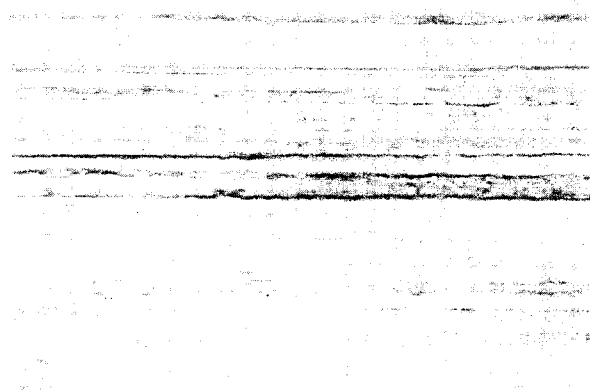The graph contains the following legend:

0.025 cm diam STABLE Nb—25% Zr WIRE
FROM SUPPLIER B, 4.2°K

O H = CONSTANT, I INCREASED
△ I = CONSTANT, H INCREASED

$\dfrac{dH}{dt} \approx 1200$ GAUSS/sec

☐ H/I = CONSTANT
◇ SOLENOID C-106, Cu-PLATED
◆ SOLENOID C-107, UNPLATED

Axis labels: $I_C(A)$ (vertical), H (kG) (horizontal)

SOLENOID C-106, PLATED

SOLENOID C-107, UNPLATED

9-16-64

2468-1505

Figure 11. Critical Currents for Short Sample Tests and Solenoids:
Stable Type B Wire

38
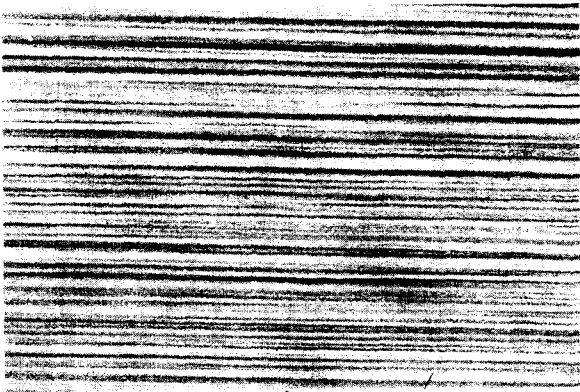
1.
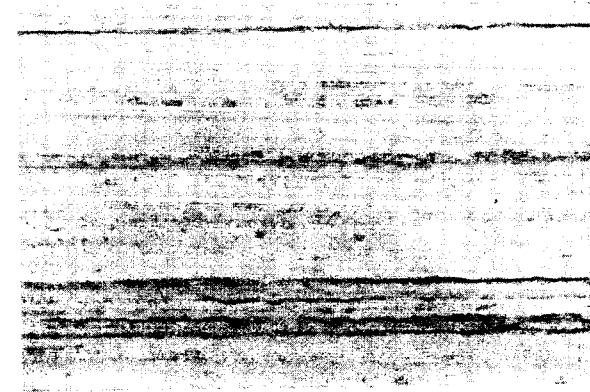SUPPLIER A
Nb—25% Zr, UNSTABLE, FROM FIGURE 6.

2.
SUPPLIER B
Nb—33% Zr, UNSTABLE, FROM FIGURE 7.

3.
SUPPLIER C
Nb—25% Zr, UNSTABLE, FROM FIGURE 8.

4.
SUPPLIER B
Nb—33% Zr, STABLE, FROM FIGURE 11.
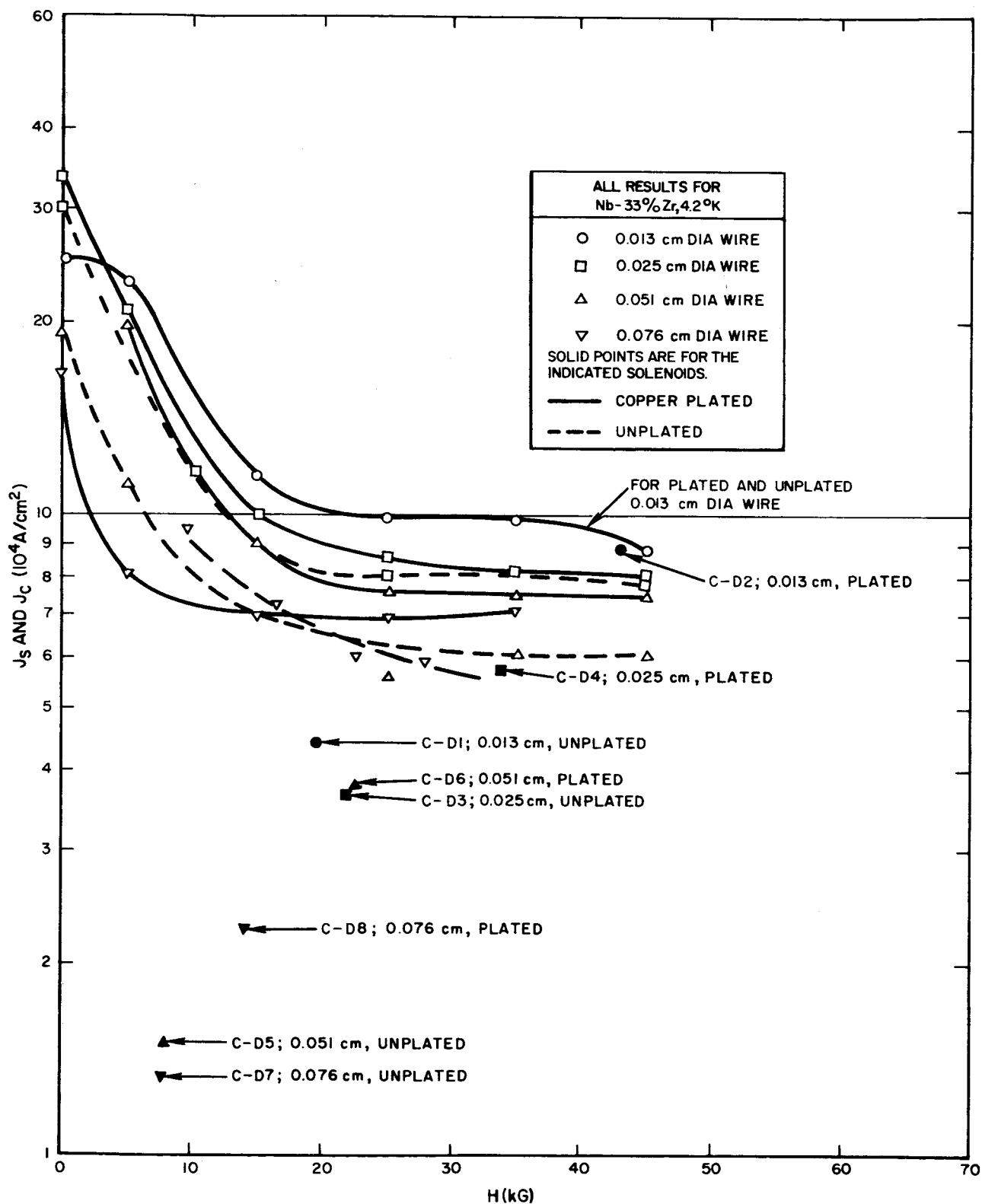
5.
SUPPLIER D
Nb—33% Zr, SEMISTABLE, FROM FIGURE 10.

ALL WIRES ETCHED WITH: 50% LACTIC, 30% HNO_3, AND 2% HF.

MAGNIFICATION = 1500X

2468-1512

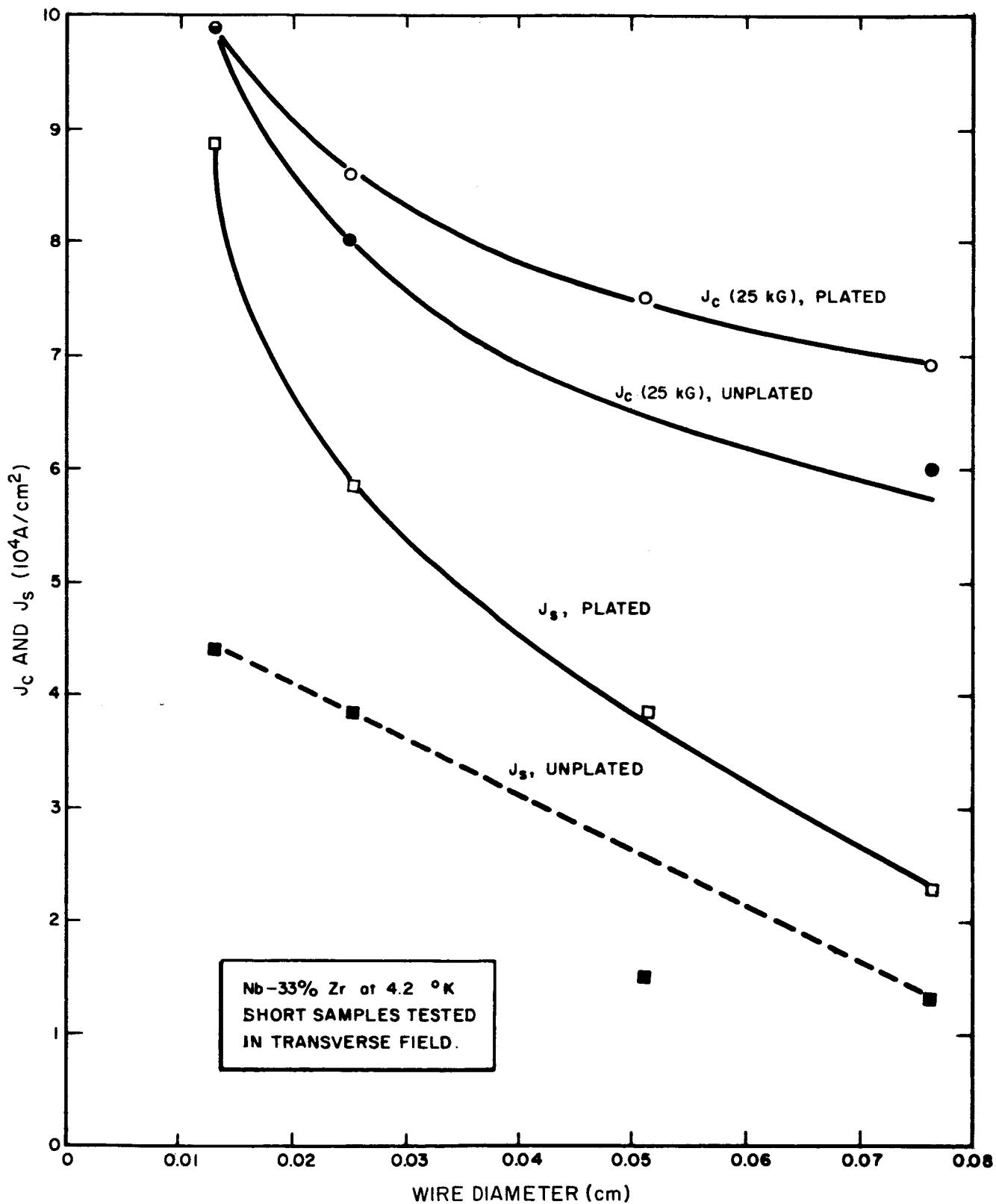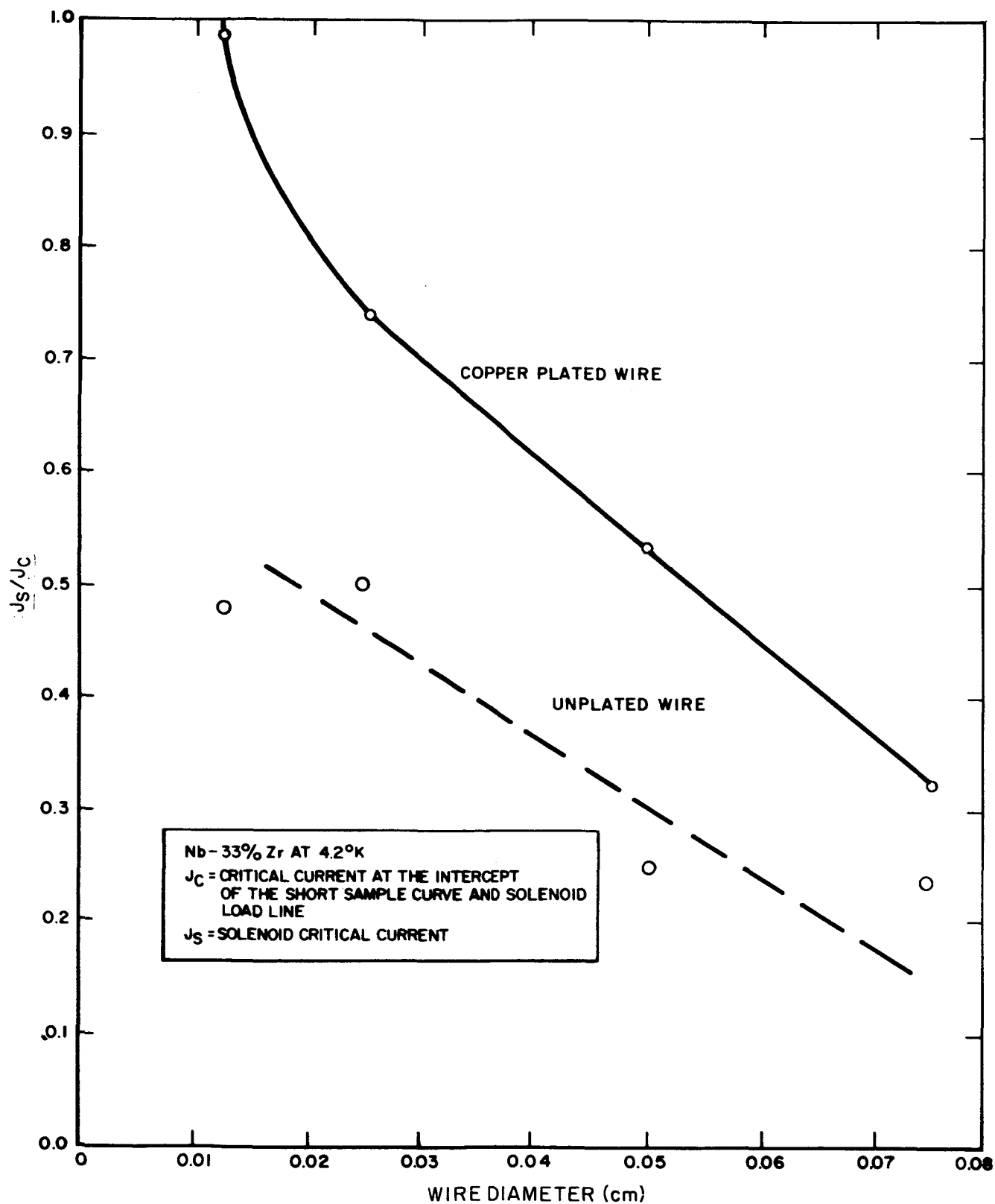Figure 12. Selected Photomicrographs of Nb-Zr Wires

Figure 13. Short Sample and Solenoid Critical Current Densities
for Different Diameter Wires
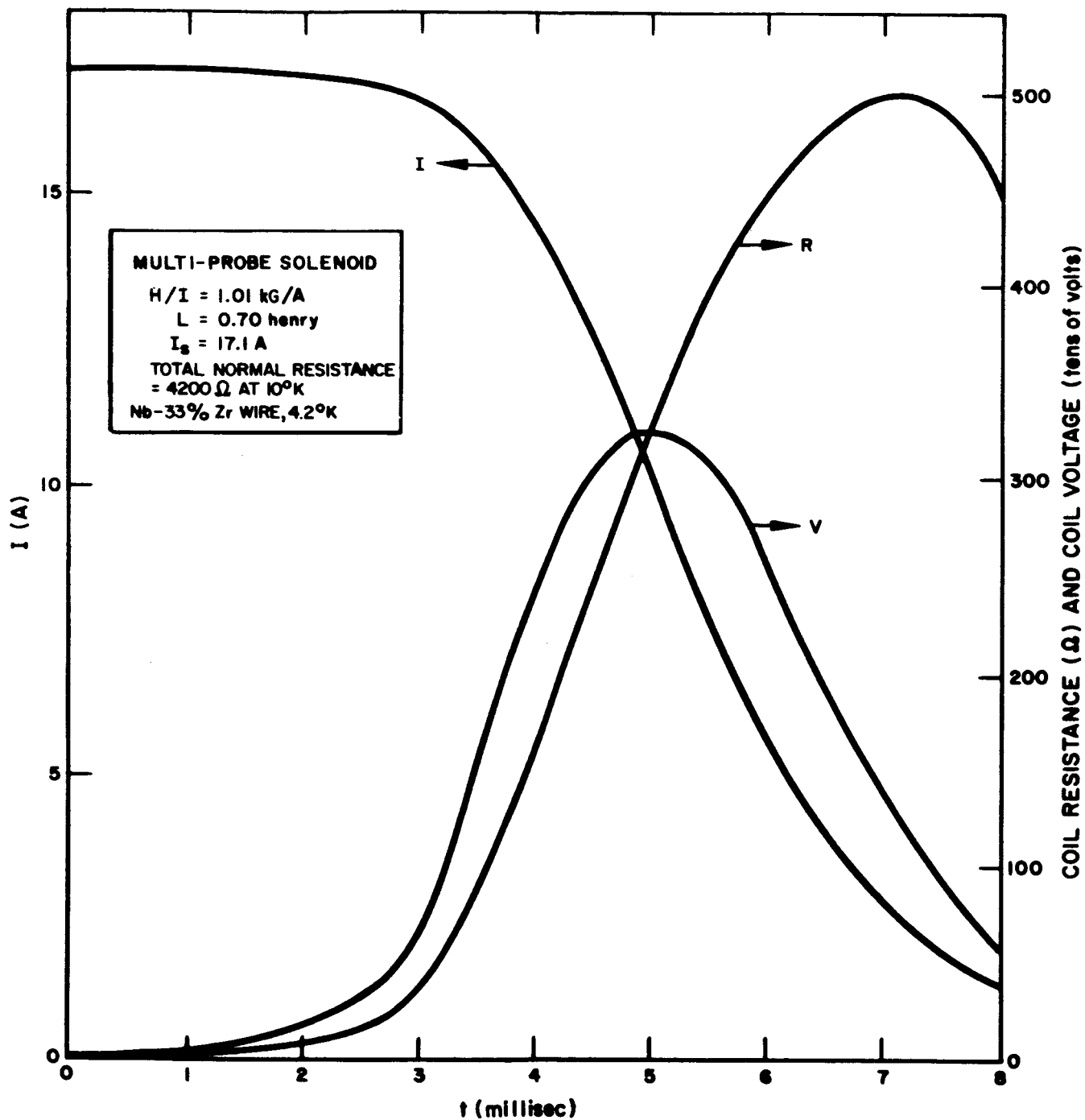
9-16-64

2468-1503

40

Figure 14. Critical Current Densities for Solenoids and Short Samples
(at 25 kG transverse) as a Function of Wire Diameter for
Copper-plated and Unplated Wire

Js/Jc

1.0
0.9
0.8
0.7
0.6
0.5
0.4
0.3
0.2
0.1
0.0

COPPER PLATED WIRE

UNPLATED WIRE

Nb - 33% Zr AT 4.2°K

Jc = CRITICAL CURRENT AT THE INTERCEPT
OF THE SHORT SAMPLE CURVE AND SOLENOID
LOAD LINE

Js = SOLENOID CRITICAL CURRENT

0   0.01   0.02   0.03   0.04   0.05   0.06   0.07   0.08
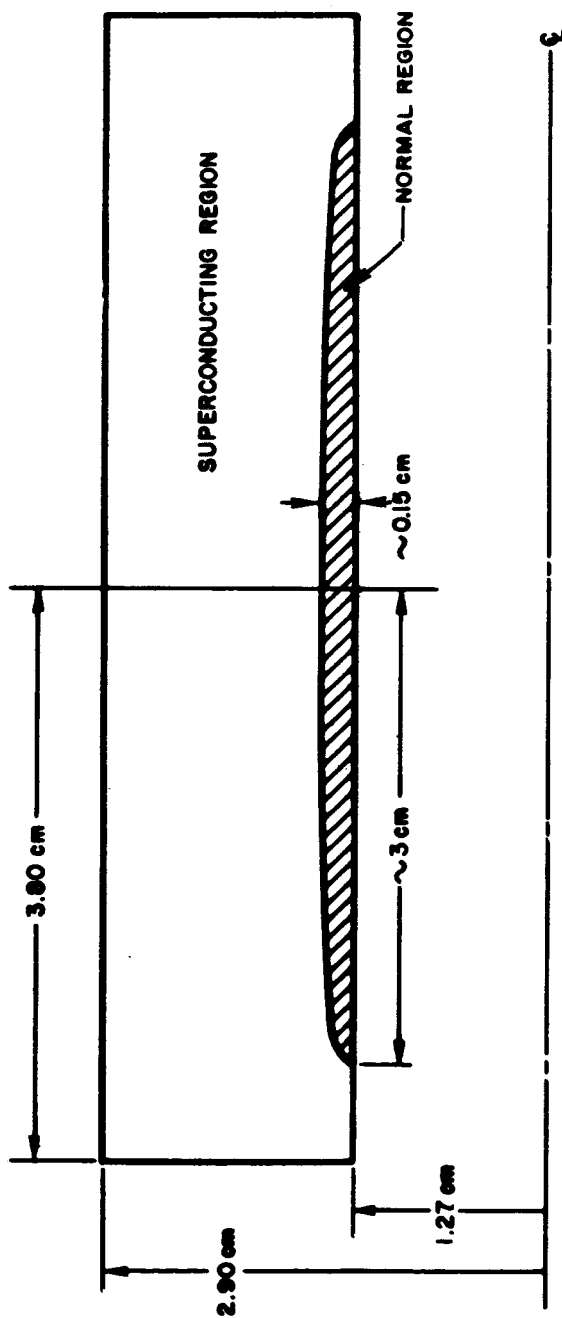
WIRE DIAMETER (cm)

9-16-64

2468-1509

Figure 15. Current Degradation for Different Diameter,
Copper-plated and Unplated Wires

42

Figure 16. Solenoid Current, Voltage, and Resistance During an SN
Transition for the Multi-probe Solenoid

SUPERCONDUCTING REGION

NORMAL REGION

~0.15 cm

3.80 cm

~3 cm

2.90 cm

1.27 cm

9-16-64

2468-1511

Figure 17. Cross Section of the Multi-probe Solenoid Normal Region for the Transition Described in Figure 16

44